Polarized luminescence for pair centres in cubic semiconductors

1991 J. Phys.: Condens. Matter 3 4731

(http://iopscience.iop.org/0953-8984/3/25/018)

J. Phys.: Condens. Matter 3 (1991) 4731–4742. Printed in the UK

Polarized luminescence for pair centres in cubic semiconductors

S S Ostapenko†
Max-Planck-Institüt für Festkörperforschung, Heisenbergstrasse 1, 7000 Stuttgart 80, Federal Republic of Germany

Received 26 November 1990, in final form 28 February 1991

Abstract. The calculations of polarization diagrams of photoluminescence for pair centres in a zincblende lattice, e.g. donor–acceptor pairs, are presented. The classical dipole approximation is applied for three types of pair spectra. The extreme values of the polarization diagram are expressed via coordinates of the corresponding pair centre in a lattice. It is possible to identify the different types of pair spectra and to provide enumeration of the pairs from their polarization characteristics. The calculations represent a theoretical basis for the new method of selectively excited polarized luminescence of pair lines.

1. Introduction

The impurity atoms as well as the native point defects (vacancies and interstitials), being introduced into a semiconductor lattice due to the doping of material or as a result of various technological treatments, often participate in the pair-centres which are characterized by discrete distances R_m between pair components. The well-known example is represented by the donor–acceptor pairs [1]. An important feature is the observation of a set of sharp spectral lines in the photoluminescence (PL), absorption or photocurrent [2] spectra. In the PL spectrum these lines arise from the optical electron transitions between the levels of donor and acceptor interacting with each other. The transition energy of each individual line is given by equation

$$h\nu_{\text{lum}}(R_m) = E_G - E_A - E_D + e^2/\varepsilon R_m - \Delta(R_m) \tag{1}$$

where E_G is the band gap energy of the semiconductor and E_A and E_D are the binding energies of the hole and electron to the isolated acceptor and donor, respectively. The last two terms describe the Coulomb and other kinds of interaction between pair components [1]. Spectrally resolved donor–acceptor pairs were investigated both in zincblende (ZB) materials GaP [3], ZnSe [4], GaAs [5] and AlSb [6] and in wurtzite materials CdS [7] and SiC [8].

Another two types of defect with discrete distributions of the centre-to-centre distances are given by nitrogen pairs in GaP [9] and Frenkel pairs, i.e. pairs of vacancy and interstitial atoms. A set of NN_i-pairs with i from 1 up to 10 was observed for nitrogen concentration in the 10^{17}–10^{18} cm^{-3} range.

† Permanent address: Institute of Semiconductors of the Ukrainian Academy of Science, pr. Nauki 45, Kiev, USSR.

0953-8984/91/254731 + 12 $03.50

Table 1. Type-I pairs.

Shell number (m)	Lattice vector $\langle a, b, c\rangle$	Local lattice symmetry	$P(0)$ π–σ	ρ	$\bar{\rho}$
1	1, 1, 0	C_{2v}	0.67–†	0.25	
2	2, 0, 0	D_{2d}	0.00–0.00	0.00	
3	2, 1, 1	C_s	0.67–0.18	0.25	
4	2, 2, 0	C_{2v}	0.67–†	0.25	
5	3, 1, 0	C_1	0.20–0.06	0.09	
6	2, 2, 2	C_{3v}	1.00–0.25	0.33	
7	3, 2, 1	E	0.67–0.18	0.25	
8	4, 0, 0	D_{2d}	0.00–0.00	0.00	
9a	4, 1, 1	C_s	0.23–0.07	0.10	0.15
9b	3, 3, 0	C_{2v}	0.67–†	0.25	
10	4, 2, 0	C_2	0.38–0.11	0.16	
11	3, 3, 2	C_s	0.92–0.24	0.32	
12	4, 2, 2	C_s	0.67–0.18	0.25	
13a	5, 1, 0	C_2	0.08–0.03	0.04	0.18
13b	4, 3, 1	E	0.67–0.18	0.25	
14	G	—	—	—	
15	5, 2, 1	E	0.33–0.10	0.14	
16	4, 4, 0	C_{2v}	0.67–(†)	0.25	
17a	5, 3, 0	C_2	0.48–0.14	0.20	0.26
17b	4, 3, 3	C_s	0.94–0.24	0.32	
18a	6, 0, 0	D_{2d}	0.00–0.00	0.00	0.24
18b	4, 4, 2	C_s	0.84–0.22	0.30	
19a	6, 1, 1	C_s	0.11–0.03	0.05	0.19
19b	5, 3, 2	E	0.67–0.18	0.25	
20	6, 2, 0	C_2	0.20–0.06	0.09	
21	5, 4, 1	E	0.67–0.18	0.25	
22	6, 2, 2	C_s	0.37–0.11	0.16	
23	6, 3, 1	E	0.42–0.12	0.17	
24	4, 4, 4	C_{3v}	1.00–0.25	0.33	
25a	7, 1, 0	C_2	0.04–0.01	0.02	22
25b	5, 5, 0	C_{2v}	0.67–†	0.25	
25c	5, 4, 3	E	0.89–0.23	0.31	

† For the $\langle a, a, 0\rangle$ dipole orientation, only π-dipoles are permitted due to selection rules for the C_{2v} group of centre symmetry [21].

Due to discrete positions in a crystal of the substitutional sites and the interstitial sites, pair centres are oriented along different but definite crystal directions with a corresponding local symmetry. We define a set of such centres as the angular-distributed-pairs (ADP). In tables 1, 2 and 3 the orientations and the local symmetry as a function of shell number (m) are presented for the type-I, type-II and type-III ADP in a ZB crystal. These three systems of the ADP cover all possible locations of substitutional sites as well as those located on cubic interstitial sites in binary ZB crystals. As shown in table 4, type-I pairs describe the location of both components on lattice sites and interstitials of the same sublattice. The position of the type-II pair components are attributed to opposite sublattices. As to the type-III pairs, their participants are those 'lattice site–interstitials' that belong to the same sublattice [10].

In fact, the atom can be replaced from the site of the ideal crystal lattice and from the geometrical centre of interstitial position as a result of bond relaxation due to the

Table 2. Type-II pairs.

Shell number (m)	Lattice vector $\langle a, b, c\rangle$	Local lattice symmetry	$P(0)$ π–σ	ρ	$\bar{\rho}$
1	1, 1, 1	C_{3v}	1.00–0.25	0.33	
2	3, 1, 1	C_s	0.37–0.11	0.16	
3	3, 3, 1	C_s	0.76–0.20	0.27	
4a	5, 1, 1	C_s	0.15–0.05	0.07	0.135
4b	3, 3, 3	C_{3v}	1.00–0.25	0.33	
5	5, 3, 1	E	0.54–0.15	0.21	
6	5, 3, 3	C_s	0.81–0.21	0.29	
7a	7, 1, 1	C_s	0.08–0.03	0.04	0.15
7b	5, 5, 1	C_s	0.70–0.19	0.26	
8a	7, 3, 1	E	0.33–0.10	0.14	0.20
8b	5, 5, 3	C_s	0.89–0.23	0.31	
9	7, 3, 3	C_s	0.55–0.15	0.21	
10a	5, 5, 5	C_{3v}	1.00–0.25	0.33	0.24
10b	7, 5, 1	E	0.60–0.17	0.23	
11a	7, 5, 3	E	0.76–0.20	0.28	0.19
11b	9, 1, 1	C_s	0.05–0.02	0.02	
12	9, 3, 1	E	0.22–0.07	0.10	
13a	9, 3, 3	C_s	0.37–0.11	0.16	
13b	7, 7, 1	C_s	0.69–0.19	0.26	0.24
13c	7, 5, 5	C_s	0.91–0.23	0.31	
14a	9, 5, 1	E	0.46–0.13	0.19	0.22
14b	7, 7, 3	C_s	0.80–0.21	0.29	
15	9, 5, 3	E	0.58–0.16	0.23	
16a	7, 7, 5	C_s	0.94–0.24	0.32	0.17
16b	11, 1, 1	C_s	0.03–0.01	0.02	
17a	9, 5, 5	C_s	0.75–0.20	0.27	
17b	11, 3, 1	E	0.15–0.05	0.07	0.18
17c	9, 7, 1	E	0.63–0.17	0.24	
18a	9, 7, 3	E	0.73–0.19	0.27	0.22
18b	11, 3, 3	C_s	0.27–0.08	0.12	
19a	11, 5, 1	E	0.34–0.10	0.15	0.18
19b	7, 7, 7	C_{3v}	1.00–0.25	0.33	
20a	11, 5, 3	E	0.44–0.13	0.18	0.24
20b	9, 7, 5	E	0.86–0.22	0.30	
21	9, 9, 1	C_s	0.68–0.18	0.25	
22a	13, 1, 1	C_s	0.02–0.01	0.01	
22b	11, 7, 1	E	0.53–0.15	0.21	0.19
22c	11, 5, 5	C_s	0.60–0.17	0.23	
22d	9, 9, 3	C_s	0.74–0.20	0.27	
23a	13, 3, 1	E	0.11–0.03	0.05	
23b	11, 7, 3	E	0.60–0.17	0.23	0.18
23c	9, 7, 7	C_s	0.94–0.24	0.32	
24a	13, 3, 3	C_s	0.20–0.06	0.09	0.195
24b	9, 9, 5	C_s	0.86–0.25	0.30	
25a	13, 5, 1	E	0.27–0.08	0.12	0.195
25b	11, 7, 5	E	0.74–0.20	0.27	

Jahn–Teller distortion, strain fields, or formation of the anisotropic centre. Thus, the axes of ADP are expected to be sensitive with respect to these anisotropic factors.

The complex structure of the pair defect induces an anisotropic electrical or local strain field leading to the polarization of corresponding optical transitions. This anisotropic field removes degeneracy of the energy levels of one or both of the pair components

Table 3. Type-III pairs.

Shell number (m)	Lattice vector $\langle a, b, c\rangle$	Local lattice symmetry	$P(0)$ π–σ	ρ	$\bar{\rho}$
1	1, 0, 0	D_{2d}	0.00–0.00	0.00	
2	1, 1, 1	C_{3v}	1.00–0.25	0.33	
3	2, 1, 0	C_2	0.38–0.11	0.16	
4	—	—	—	—	
5a	2, 2, 1	C_s	0.86–0.22	0.30	0.24
5b	3, 0, 0	D_{2d}	0.00–0.00	0.00	
6	3, 1, 1	C_s	0.38–0.11	0.16	
7	3, 2, 0	C_2	0.52–0.15	0.21	
8	—	—	—	—	
9a	4, 1, 0	C_2	0.13–0.04	0.06	0.18
9b	3, 2, 2	C_s	0.86–0.22	0.30	
10	3, 3, 1	C_s	0.74–0.20	0.27	
11	4, 2, 1	E	0.47–0.14	0.19	
12	—	—	—	—	
13a	5, 0, 0	D_{2d}	0.00–0.00	0.00	0.18
13b	4, 3, 0	C_2	0.60–0.17	0.23	
14a	5, 1, 1	C_s	0.15–0.05	0.07	0.135
14b	3, 3, 3	C_{3v}	1.00–0.25	0.33	
15a	5, 2, 0	C_2	0.27–0.08	0.12	0.23
15b	4, 3, 2	E	0.82–0.21	0.29	
16	—	—	—	—	
17a	4, 4, 1	C_s	0.74–0.20	0.27	0.235
17b	5, 2, 2	C_s	0.50–0.14	0.20	
18	5, 3, 1	E	0.52–0.15	0.21	
19	6, 1, 0	C_2	0.06–0.02	0.03	
20	—	—	—	—	
21a	6, 2, 1	E	0.25–0.08	0.11	0.195
21b	5, 4, 0	C_2	0.63–0.17	0.24	
21c	4, 4, 3	C_s	0.94–0.24	0.32	
22	5, 3, 3	C_s	0.82–0.21	0.29	
23a	5, 4, 2	E	0.82–0.21	0.29	0.25
23b	6, 3, 0	C_2	0.38–0.11	0.16	
24	—	—	—	—	
25a	7, 0, 0	D_{2d}	0.00–0.00	0.00	0.19
25b	6, 3, 2	E	0.52–0.15	0.21	

and thus reduces the pair symmetry. In the case of shallow donor–acceptor pairs it has been shown that the polarization of emission of the individual pair results from the splitting of the degenerate hole level by the Coulomb donor field [11]. In the case of nitrogen pairs their low symmetry, attributed to the anisotropic field of the defect, has been revealed [12]. The optical anisotropy of a complex centre can be investigated by methods of polarization spectroscopy [13] that involve piezospectroscopy, induced linear dichroism, Stark, Zeeman and Faraday effects as well as the polarized luminescence. The last is known also as the method of polarization diagrams (PD). It is based on selective polarized excitation of the PL centre and measurement of its induced

Table 4. The combination of pairs of A and B atoms in a ZB lattice that give rise to the three types of pair spectra. A_s and B_s are substitutional sites; A_i and B_i are cubic interstitial sites.

Type-I	Type-II	Type-III
A_s–A_s	A_s–B_s	A_s–A_i
A_i–A_i	A_i–B_i	B_s–B_i
B_s–B_s	A_s–B_i	
B_i–B_i	B_s–A_i	

polarization degree (see below). The PD method was elaborated and applied for the first time to associated complex defects in dielectric crystals [14]. Later it was developed theoretically for anisotropic semiconductors [15, 16] and recently generalized for the two-dipole [17] and multipole [18] approximation. The experimental simplicity of the PD method and the possibility of investigating both sharp and broad spectral lines makes it attractive.

The theory of the PD method was previously developed for the centres oriented along ⟨100⟩, ⟨111⟩ and ⟨110⟩ directions in cubic crystals [16], which are specified in a ZB lattice by D_{2d}, C_{3v} and C_{2v} symmetry, respectively. The application of the PD method for the ADP is impeded, however, by the absence of calculations for the pair centres with the arbitrary orientation in a lattice and the local symmetry lower than C_{2v}, i.e. C_2, C_s and E. In fact, just these centres are responsible for the majority of ADP, as one can see from the tables 1, 2 and 3.

In this paper the polarized luminescence of the ADP in cubic ZB crystals is for the first time considered theoretically in the framework of the classical dipole approximation. The PDs of the pair centres oriented along arbitrary crystal directions are calculated and classified. The analytic relationship between PD extreme points and lattice coordinates of the pair centre is derived. The strong dependence of the PD characteristics on the pair number is predicted for each type of ADP. The latter enables one to accept this technique as the new method of selectively exciting polarized luminescence of the angular distributed pairs in cubic semiconductors.

2. The basis of the PD method

The PD method applied to cubic crystals is based on selective excitation by linearly polarized light of the orientationally degenerate anisotropic PL centres treated as classical dipoles [14]. The resulting luminescence demonstrates linear polarization due to the removal of the orientational degeneracy of these dipoles. The PL polarization degree, P, is a function of the dipole direction and depends on the angle, φ, of the polarization plane of an exciting light, E_{ex}, with respect to the chosen crystal axis. The PD is defined as having the following angular dependence:

$$P(\varphi) = [I_{\parallel}(\varphi) - I_{\perp}(\varphi)]/[I_{\parallel}(\varphi) + I_{\perp}(\varphi)] \tag{2}$$

where $I_{\parallel}(\varphi)$ and $I_{\perp}(\varphi)$ are the intensities of two orthogonally polarized PL components when the polarization plane of the luminescence analyser is oriented correspondingly parallel, $E^{\parallel}_{lum}$, and perpendicular, $E^{\perp}_{lum}$, to the electric field vector of the exciting light

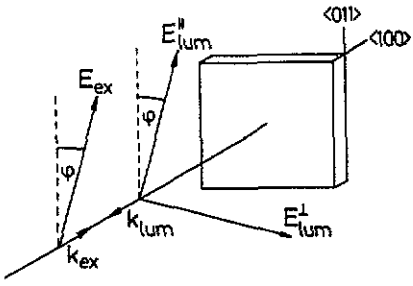

Figure 1. The scheme for the polarized luminescence measurements. E_{ex} and E_{lum} are the electric field vectors of the exciting light and of the luminescence, k_{ex} and k_{lum} are their wave vectors. The sample is oriented in (100) plane.

(figure 1). It is supposed that the directions of the exciting light propagation and of the PL recording are parallel, that is the case in our study; alternatively, they can be perpendicular one to another. The final numerical results depend on the chosen PL registration scheme. However, they can be easily adapted to the case of practical interest using the method proposed. By measuring the complete curve of the PD and comparing it with the developed theory, one can determine the orientations of both emitting and absorbing optical dipoles as well as the type of dipole transition [17].

In the experiment the optical anisotropy of the PL centre is demonstrated by observation of the PL 'induced polarization'. The latter means the fulfilment of at least one of two inequalities for the PD extreme points:

$$P(0) = P(\pi/2) \neq 0 \qquad P(\pi/4) = P(3\pi/4) \neq 0. \tag{3}$$

As will be shown below, the values of $P(0)$ and $P(\pi/4)$ are sensitive to the centre orientation in a lattice.

The important peculiarity of the PD method has to be underlined: excitation of the PL band with light of frequency above that of the band-gap results in the absorption of all anisotropic centres independently of their orientation and, hence, leads to the unpolarized luminescence. Consequently, to apply the PD method, polarized excitation has to be performed in the absorption maximum corresponding to the chosen PL band. In the case of ADP luminescence, this selective excitation of the individual pair line is provided by resonance excitation using time-resolved measurements [19] or alternatively via the excited states of the centre [20]. A technique of selective PL excitation is suitable for these measurements.

3. Calculations

To calculate the PD of the pair centre in a ZB crystal the following are assumed:

(i) The electrical dipole transitions dominate the light absorption and emission. Due to this the multipole terms can be neglected and the classical dipole approximation is utilized;

(ii) The direction of the absorption dipole coincides with that of the emitting dipole (one-dipole model) as a result of direct pair excitation;

(iii) This direction also coincides with the pair-centre axis given by a vector $\langle a, b, c\rangle$;

(iv) The pair centres are affected by orientation degeneracy, i.e. occupy symmetry-equivalent orientations with equal probability. The symmetry-equivalent orientations

in a ZB lattice are given by changing the sequence of a, b and c and their sign in accordance with the symmetry operation of the T_d group;

(v) The optical transitions represent a superposition of oscillator (π) and rotator (σ) and are characterized by the parameter β [17]. The value of β is changed in the range of $0 \leqslant \beta \leqslant 1$ as a result of the variation of the π/σ-dipole ratio and is 0 for a 'pure' π-dipole and 1 for a 'pure' σ-dipole. To simplify the final result of calculations, the value of β is supposed to be the same for excitation and luminescence transitions, $\beta_{ex} = \beta_{lum}$.

This consideration of optical transition in a model of π and σ dipoles is based on selection rules of group theory [21]. The allowed dipole transitions are given by irreducible representations of the symmetry group of a particular centre. For instance, the centre of C_{3v} symmetry possesses A_1, A_2 and E representations. Thus, the $A_1 \Rightarrow A_2$ transition is described by a π-dipole along the $\langle 111 \rangle$ centre axis, while the $A_1 \Rightarrow E$ transition is attributed to a σ-dipole in a plane perpendicular to the same $\langle 111 \rangle$ axis. If corresponding spectral bands are overlapped (e.g. due to temperature or electron–phonon broadening), then both transitions can be observed simultaneously and the model of superposed π/σ dipoles is valid. This suggestion is illustrated by experiments on the symmetry of deep centres in ZnS [22]. It should be noted that in the case of a centre with C_{2v} symmetry, only π dipoles are allowed and hence, no σ dipoles can be involved in the theory. This fact is reflected in table 1 for corresponding $\langle a, a, 0 \rangle$ orientations.

We consider the PL to be excited in and measured from the (100) crystal plane while the angle φ is relative to the $\langle 011 \rangle$ axis (figure 1). This crystal plane provides the highest 'induced polarization' degree of the PL as compared with others [14]. Evidently, the results of computations are linked to this experimental geometry. The general relation for intensities of two orthogonally polarized PL components, $I_\parallel$ and $I_\perp$, for the π-dipole is given by

$$I_{\parallel,\perp}(\varphi) = \sum_\nu |E_{ex}(\varphi) \cdot e_\nu|^2 |E^{\parallel,\perp}_{lum}(\varphi) \cdot e_\nu|^2 \tag{4}$$

where summation is over all symmetry-equivalent dipole orientations and e_ν denotes the unit vector of the dipole direction. The same expression (4) holds in the case of the σ dipole if e_ν is replaced by a unit vector which rotates in a plane perpendicular to the dipole direction [15]. The following expression for the PD of orientationally degenerate dipoles $\langle a, b, c \rangle$ is derived from (4)

$$P(\varphi) = (1 - 2\beta)^2[(1 - 3\rho)\sin^2 2\varphi + 2\rho \cos^2 2\varphi]/[1 + 2\beta^2 - (1 - 2\beta)^2\rho] \tag{5}$$

$$\rho = (a^2b^2 + b^2c^2 + a^2c^2)/(a^2 + b^2 + c^2)^2. \tag{6}$$

In figure 2(a) the PDs are shown for the pairs oriented along $\langle 100 \rangle$, $\langle 111 \rangle$ and $\langle 110 \rangle$ directions that have been calculated in [14]. The PD family for some of the type-I pairs is plotted, using (5)–(6), in figure 2(b). It demonstrates the strong change of the PD amplitude as a consequence of different orientation of the corresponding dipoles in a crystal lattice.

The PD of various pairs can be classified using the orientational parameter ρ, which is defined by (6) and shown for each type of ADP in tables 1–3. The value of ρ is linked to the pair orientation and is changed in the range $0 \leqslant \rho \leqslant \frac{1}{3}$. The following relation of the PD extreme points, $|P(0)| \geqslant |P(\pi/4)|$, is valid when $0.2 \leqslant \rho \leqslant \frac{1}{3}$, while inverse inequality, $|P(0)| \leqslant |P(\pi/4)|$, occurs for $0 \leqslant \rho \leqslant 0.2$. The limiting cases correspond to the dipoles along $\langle 100 \rangle$ axes ($\rho = 0$) and $\langle 111 \rangle$ axes ($\rho = \frac{1}{3}$), figure 2(a).

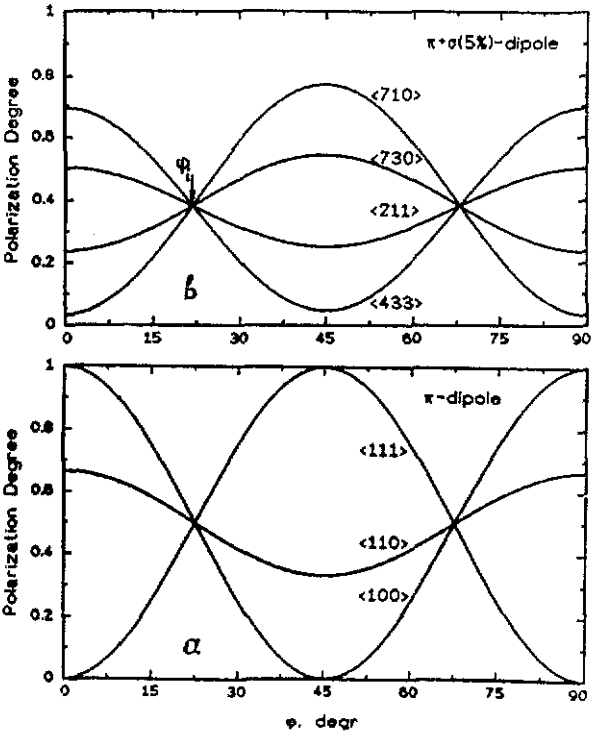

Figure 2. The PD curves for (*a*) the dipoles aligned along the main cubic directions [14] and (*b*) for some of the type-I ADP. The angle φ_i is related to the value of β for the pairs with equal β values.

As will be shown below, the coordinates of the ADP dipole can be related to the values of $P(0)$ and $P(\pi/4)$. The expressions for the $P(0)$ and $P(\pi/4)$ are derived from (5) as follows:

$$P(0) = (1 - 2\beta)^2(2\rho)/[1 + 2\beta^2 - \rho(1 - 2\beta)^2] \tag{7}$$

$$P(\pi/4) = (1 - 2\beta)^2(1 - 3\rho)/[1 + 2\beta^2 - \rho(1 - 2\beta)^2]. \tag{8}$$

The computed $P(0)$ values of the type-I, II and III ADP for the π and σ dipoles are shown in tables 1–3. These values define the range of the $P(0)$ variation if β is changed within limits $0 \leqslant \beta \leqslant 1$. The corresponding range for the $P(\pi/4)$ value can be calculated from equation (8). The curves of $P(0)$ as a function of β are plotted in figure 3 for some pairs.

It should be noted that definite pairs are characterized by the same shell number m, possessing, however, different orientations as shown by brackets in tables 1, 2 and 3. This is the case for type-I pairs with $m = 9$, 13, 17–19 and 25, for type-II pairs with $m =$ 4, 7, 8, 10, 11, 13, 14, 16–20 and 22–25 and for type-III pairs with $m = 5$, 9, 13–15, 17, 21, 23 and 25. If the transition energies are weakly affected by anisotropic interaction between pair components [1], then the lines of the pairs with the same shell number are unresolved in the PL spectrum. For these lines the calculated degree of polarization, $P(0)$, is averaged at the polarizations of the individual sublines. The results of the averaging are presented for the corresponding lines in figure 4 by special labels along with the data for non-degenerate pairs. It is worth noticing that averaging the $P(0)$

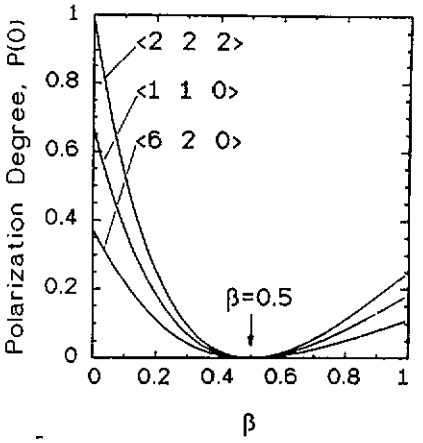

Figure 3. The dependence of the $P(0)$ value on β for three pairs. The case of $\beta = 0.5$, the portions of π dipole and σ dipole in luminescence and excitation are equal.

values on pairs with various orientations in a ZB lattice reduces the difference in the corresponding PL polarization degree. If the superposition of lines with the same m is removed in the PL spectrum, then each subline is specified by its own $P(0)$ value, as shown in tables 1–3. An example of such 'polarization splitting' is demonstrated in figure 4(a) for the pair with $m = 9$, being a superposition of two pairs oriented along ⟨411⟩ and ⟨330⟩ axes.

The results presented in figure 4 show the strong variation of the $P(0)$ value from one pair to another as well as between different types of ADP. In particular, some of the pair lines possess near extreme $P(0)$ values. In fact, the magnitude of $P(0)$ reaches 0.74–1.0 for pairs with $m_{\mathrm{I}} = 6$, 11 and 24 (type-I), $m_{\mathrm{II}} = 1$, 3 and 6 (type-II) and $m_{\mathrm{III}} = 2$, 10 and 22 (type-III), while it is equal to 0–0.25 for $m_{\mathrm{I}} = 2$, 5, 8 and 20, $m_{\mathrm{II}} = 12$ and $m_{\mathrm{III}} = 1$ and 19. Thus, the polarization of these pair lines can be used as a method of distinguishing different sets of ADP and of providing their correct numbering.

The analysis shows that the dependence of $P(0)$ on the shell number presented in figure 4 is maintained if all pairs possess the same β value, i.e. characterized by the equal superposition of π and σ dipoles. Only the scale of $P(0)$ will be affected. To check if this is the case for a given system of ADP, one can measure the complete PD curve of different pair lines and evaluate the angles of intersection, φ_i, (figure 2). This angle has to be the same for the set of pairs with equal β values. In fact, the angle φ_i is unambiguously related to the value of β as follows:

$$\tan 2\varphi_i = (1 + 2\beta^2)/(1 + \beta)^2. \tag{9}$$

However, the value of φ_i is changed from 19.6° to 22.5° only when $0 \leqslant \beta \leqslant 1$, as follows from (9). Evidently, this range is too narrow to allow the evaluation of a reliable value of β, taking into account experimental inaccuracy that is usually of the order of 1°.

To exclude the influence of β on the polarization of ADP the following relation between PD extreme points and the coordinates of the corresponding dipole is derived from (7)–(8):

$$\rho = (a^2b^2 + b^2c^2 + a^2c^2)/(a^2 + b^2 + c^2)^2 = P(0)/[3P(0) + 2P(\pi/4)]. \tag{10}$$

The right hand side of (10) includes only experimental points of the PD as its extrema $P(0)$ and $P(\pi/4)$, while the dipole coordinates are assembled in the left hand side of (10). In figure 5 and tables 1–3, calculated values of ρ for each type of pair, and $\bar{\rho}$

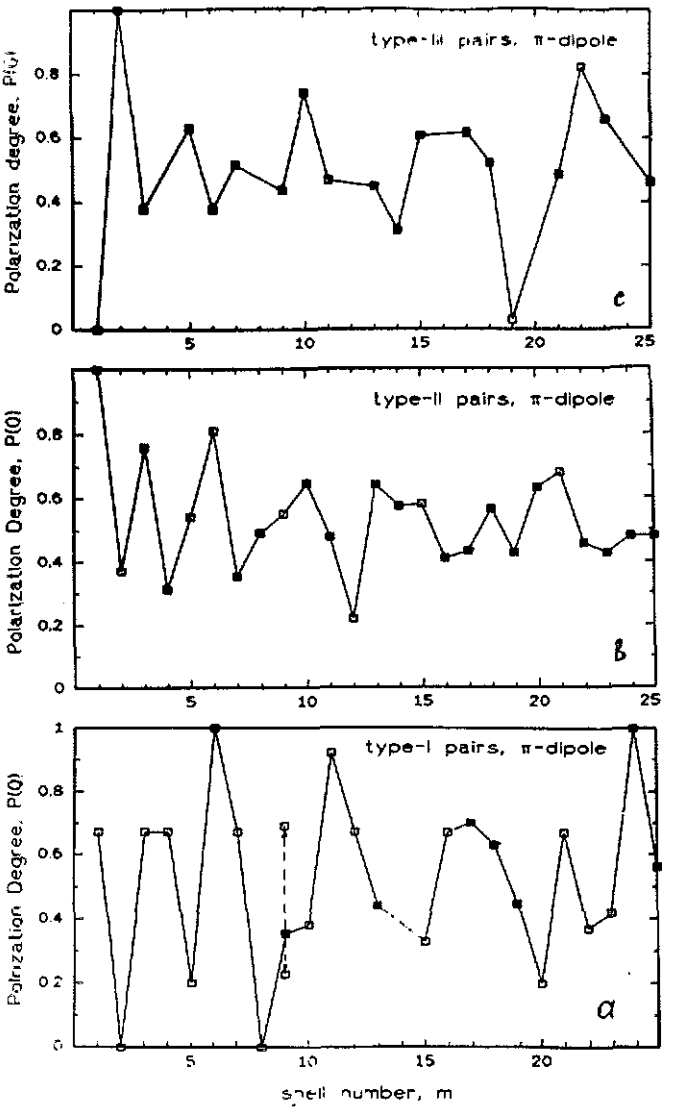

Figure 4. The shell number dependence of the $P(0)$ value for the (*a*) type-I, (*b*) type-II and (*c*) type-III pairs. The case of $\beta = 0$ is presented. The pairs with the shell degeneration are marked by (■).

corresponding to pairs with shell degeneration are presented. It is remarkable that the value of ρ is β-free even if one assumes a different value of β in excitation and luminescence, i.e. $\beta_{ex} \neq \beta_{lum}$. Thus ρ dependence on m can be taken to be the 'finger print' for the corresponding system of ADP. Thus, the comparison of the experimental $\rho(m)$ dependence and the calculated one (figure 5) enables one to identify the ADP system (type-I, II or III) and to determine the real orientation of the individual pair centre. It is also useful, evidently, to use (10) to demonstrate the difference in dipole orientations for some of the pair lines characterized by various ρ magnitudes.

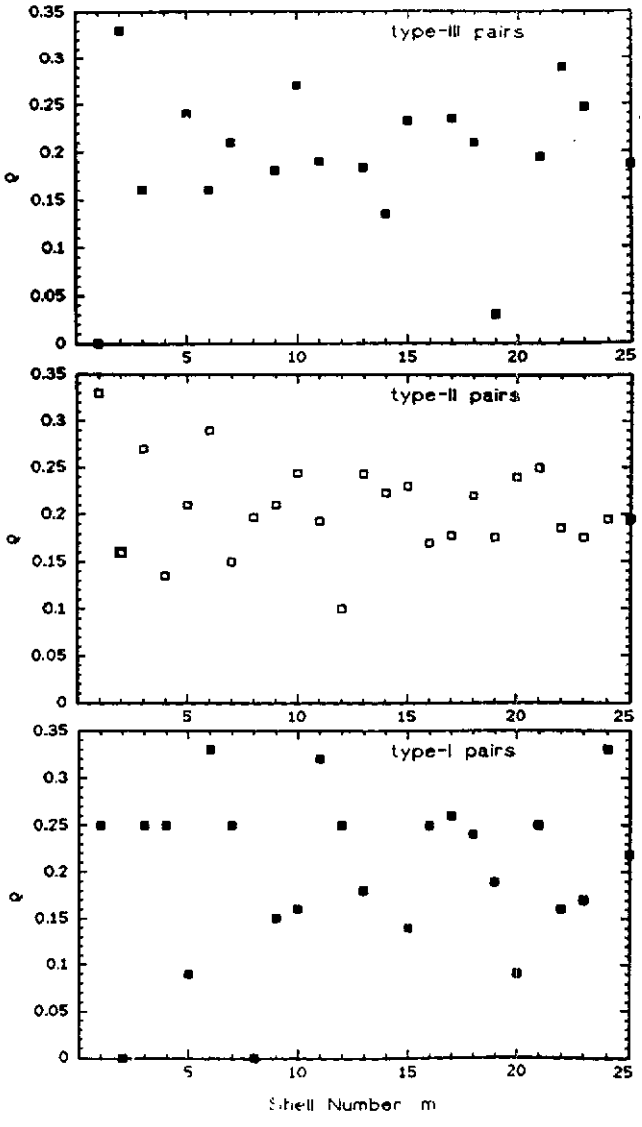

Figure 5. The shell-number dependence of the orientation parameter ρ and its averaged value, $\bar{\rho}$, for three types of ADP.

4. Conclusions

The measurements of the polarization diagram of the discrete pair lines in a ZB lattice semiconductor can provide:

(i) the manifestation for the pair optical anisotropy and their different orientation in a crystal lattice;

(ii) the quantitative information about coordinates of the corresponding optical dipoles by fitting the value of ρ to the experimental PD extreme points (ratio (10));

(iii) the proof of the accuracy of pair numbering.

The latter is especially important for the closely spaced pair components when the shift of the optical transition energy is not described by a simple Coulomb relation due to the increase of the short-range interaction term $\Delta(R_m)$ in (1).

It should be noted that the relation (10) is valid only if the orientation of the pair centre in a crystal lattice coincides with the direction of absorbing and emitting optical dipoles, as assumed above. This condition can be violated when the polarization of the optical transition results from other factors such as internal stress fields or low symmetry of pair components.

The calculations presented form the theoretical background for the application of the new method of selectively excited polarized luminescence of angularly distributed pairs in ZB semiconductors. The theory was applied recently to the donor–acceptor pair luminescence in AlSb crystals [23]. The experiments on GaP pair lines are in progress.

Acknowledgments

I would like to thank Professor M K Sheinkman, Dr H J von Bardeleben, Dr I A Buyanova and Dr G Hofmann for the critical reading of the manuscript and helpful discussions. The author acknowledges the support of the Alexander von Humboldt Foundation in its partial financing of this work.

References

[1] Dean P J 1973 *Progress in Solid State Chemistry* vol 8, ed J Q McCaldin and G Somorgai (Oxford: Pergamon) pp 1–126
[2] Rizachanov M A 1976 *Sov. Phys.–Semicond.* **10** 1357
[3] Dean P J, Henry C H and Frosch C J 1968 *Phys. Rev.* **168** 812
[4] Tews H, Venghaus H and Dean P J 1979 *Phys. Rev.* B **19** 5178
[5] Reynolds D C, Bajaj K K, Litton C W, Smith E B, Yu P W, Masselink W T, Fisher F and Mazkos H 1984 *Solid State Commun.* **52** 685
[6] Lorenz M R, Morgan T N, Pettit G D and Turner W J 1968 *Phys. Rev.* **168** 902
[7] Henry C H, Faulkner R A and Nassau K 1969 *Phys. Rev.* **183** 798
[8] Choyke W J, Hamilton D R and Patrick L 1964 *Phys. Rev.* **133A** 1163
[9] Thomas D J and Hopfield J J 1966 *Phys. Rev.* **150** 680
[10] Ryan F M and Miller R C 1966 *Phys. Rev.* **148** 858
[11] Baru V G, Petrov V A and Sandomirskii V B 1975 *Sov. Phys.–Semicond.* **9** 1344
[12] Gil B, Camassel J, Albert J P and Mathieu H 1986 *Phys. Rev.* B **33** 2690
[13] Kaplyanskii A A and Feofilov P P 1962 *Sov. Phys.–Usp.* **5** 79
[14] Feofilov P P 1961 *The Physical Basis of Polarized Emission* (New York)
[15] Bukke E E, Grigor'ev N N and Fok M V 1974 *Trudi Fiz. Inst. Akad. Nauk.* **79** 108 (in Russian)
[16] Ostapenko S S, Tanatar M A and Sheinkman M K 1980 *Opt. Spectrosc.* **48** 430
[17] Buyanova I A, Oborina E I and Ostapenko S S 1989 *Semicond. Sci. Technol.* **4** 797
[18] Kisilyuk A A and Ostapenko S S 1987 *Dep. VINITI, No* 2259-B88 p 20 (in Russian)
[19] Kisilyuk A A, Ostapenko S S and Sheinkman M K 1987 *Opt. Spectrosc.* **62** 657
[20] Senske W and Street R A 1979 *Phys. Rev.* B **20** 3267
[21] Kaplyanskii A A 1964 *Opt. Spectrosc.* **64** 602
[22] Mochnyak J 1978 *J. Lumin.* **16** 61
[23] Ostapenko S S and Hofmann G 1990 *Solid State Commun.* **74** 447